Electronic Supplementary Material (ESI) for Physical Chemistry Chemical Physics.

Supporting Information

Functional ionic liquid for enhancement of Li-ion transfer: Effect of cation structure on charge−discharge performance of $Li_4Ti_5O_{12}$ electrode

Masahiro Shimizu,[ab] *Hiroyuki Usui,*[ab] *and Hiroki Sakaguchi*[ab]*

[a]*Department of Chemistry and Biotechnology, Graduate School of Engineering, Tottori University*
4-101 Minami, Koyama-cho, Tottori 680-8552, Japan

[b]*Center for Research on Green Sustainable Chemistry, Tottori University*
4-101 Minami, Koyama-cho, Tottori 680-8552, Japan

*Corresponding author. Tel./Fax: +81-857-31-5265; e-mail: sakaguch@chem.tottori-u.ac.jp

Electrode preparation by a gas-deposition method

In the preparation of $Li_4Ti_5O_{12}$ thick-film electrodes by a gas-deposition method, commercial $Li_4Ti_5O_{12}$ powder (99%, Aldrich) was used as the raw material. For the gas-deposition, a Cu current collector (20-μm thickness, 99.9%, Nilaco Co., Ltd.) was placed at a distance of 10 mm from the nozzle in a vacuum chamber with a guide tube. The nozzle with a 0.3 mm diameter was connected to the end of the guide tube. A helium carrier gas with a purity of 99.9999% (6N) was used at a differential pressure of 8.0×10^5 Pa. After the chamber had been evacuated to a base pressure of several ten Pa, an aerosol consisting of the helium carrier gas and the $Li_4Ti_5O_{12}$ powder was generated in the guide tube, and instantly gushed from the nozzle onto the Cu substrate. The weight of the deposited active material on the substrate was measured to an accuracy of 1 μg by ultra-microbalance (XP6, METTLER TOLEDO) equipped with an anti-vibration table.

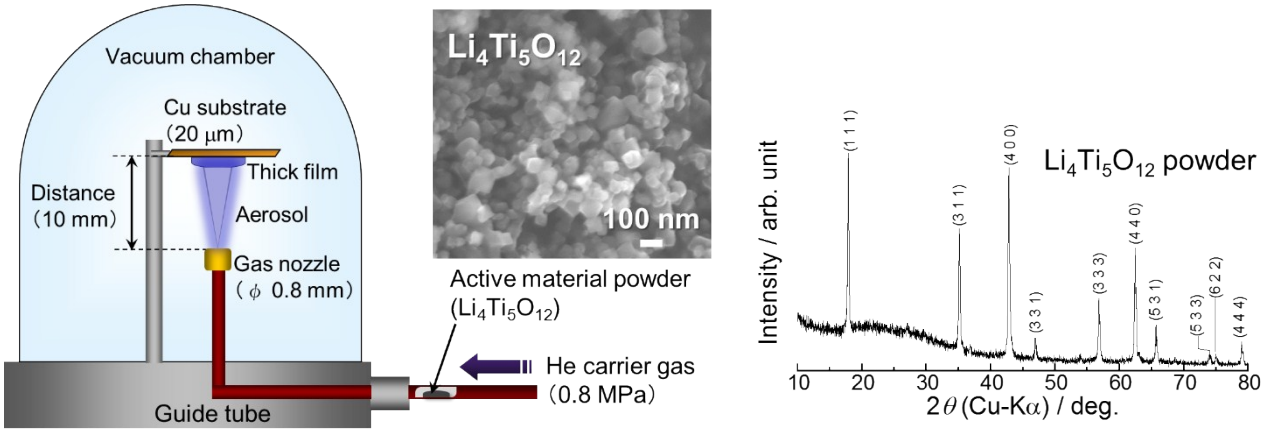

Figure S1. (left) Schematic illustration for preparation of thick-film electrodes using a gas-deposition method. In this study, $Li_4Ti_5O_{12}$ powder with a diameter of 100 nm was used as the active material. (right) XRD pattern of the $Li_4Ti_5O_{12}$ powder used in this study.

Physicochemical properties of piperidinium-based ionic liquids and electrolytes

The electrical conductivity was investigated by an electrochemical impedance measurement (CompactStat, Ivium Technologies) through the use of the cell equipped with two Pt electrodes under argon atmosphere at various temperatures from 293 to 353 K. A thermogravimetric (TG) analysis was conducted to determine thermal decomposition temperature of ionic liquids by using a TG analyzer (Thermo plus EVO II, Rigaku Co., Ltd.) with a heating rate of 10 °C min^{-1} from ambient temperature to 500 °C under argon atmosphere.

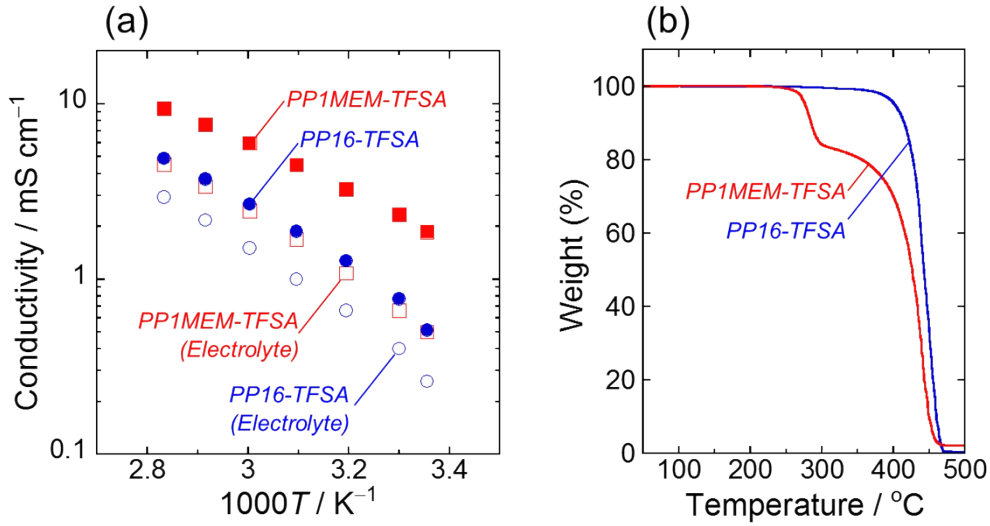

Figure S2. (a) Temperature dependence of conductivity of neat ionic liquids and ionic liquid electrolytes. (b) Thermogravimetric traces for the ionic liquids of PP1MEM-TFSA and PP16-TFSA.

Table S1. Summary of physicochemical properties of TFSA-based ionic liquids synthesized in this study. The electrolytes were prepared by dissolving of LiTFSA with a concentration of 1.0 M.

Cation	M.W. [a]	η [b] / mPa s	σ [c] / mS cm^{-1}	σ [c] / mS cm^{-1}	T_{dec} [d] / °C
PP1MEM	468	69	2.3	0.7	285
PP16	464	132	0.8	0.4	415

[a] Molecular weight
[b] Viscosity at 303 K
[c] Conductivity at 303 K
[d] Thermal decomposition temperature (10% weight loss)

Raman spectra of $(LiTFSA)_x(Ionic\ liquid)_{1-x}$ solutions

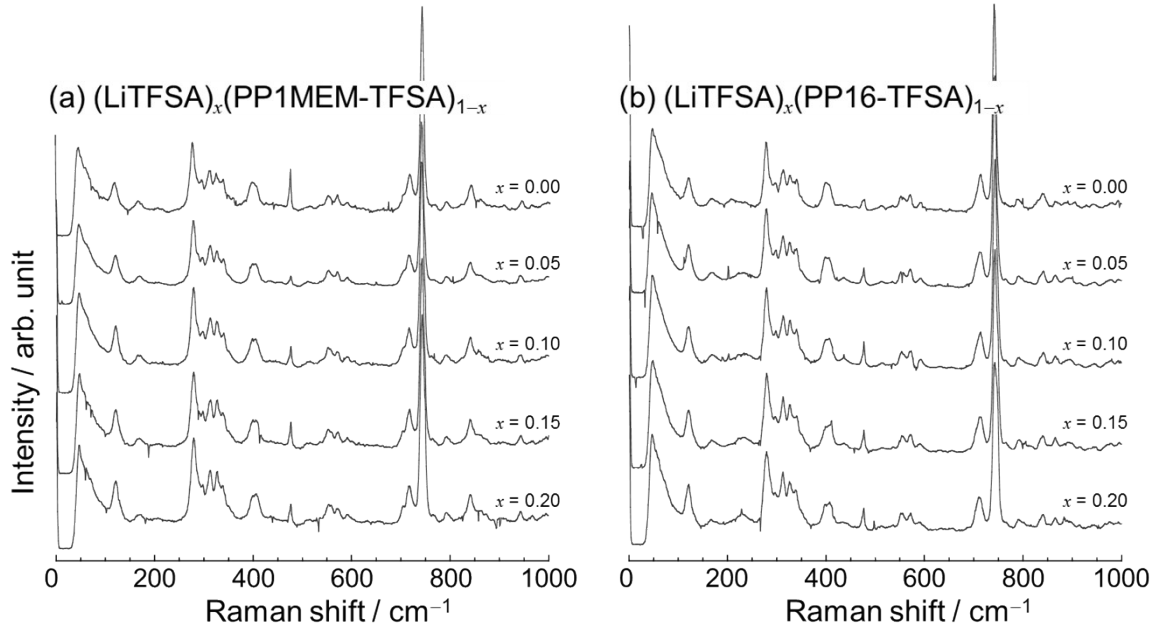

Figure S3. Raman spectra of (a) $(LiTFSA)_x(PP1MEM\text{-}TFSA)_{1-x}$ and (b) $(LiTFSA)_x(PP16\text{-}TFSA)_{1-x}$ solutions (x = 0, 0.05, 0.10, 0.15, 0.20) in the frequency range of 0 to 1000 cm^{-1}.

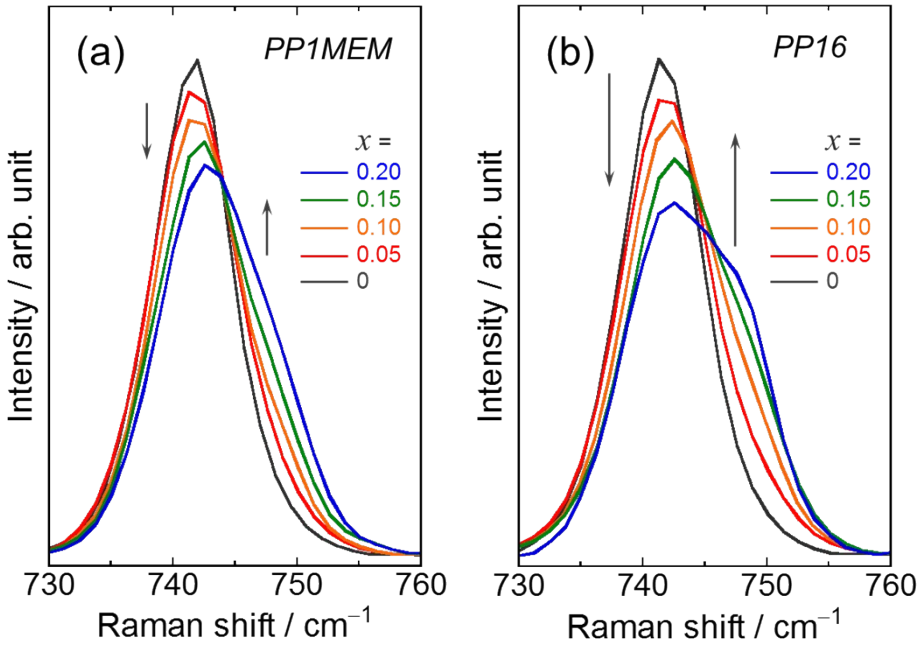

Figure S4. Raman spectra of (a) $(LiTFSA)_x(PP1MEM\text{-}TFSA)_{1-x}$ and (b) $(LiTFSA)_x(PP16\text{-}TFSA)_{1-x}$ solutions (x = 0, 0.05, 0.10, 0.15, 0.20) in the frequency range of 730 to 760 cm^{-1}.

Raman spectra of $(DME)_x(LiTFSA)_{1-x}$ solutions

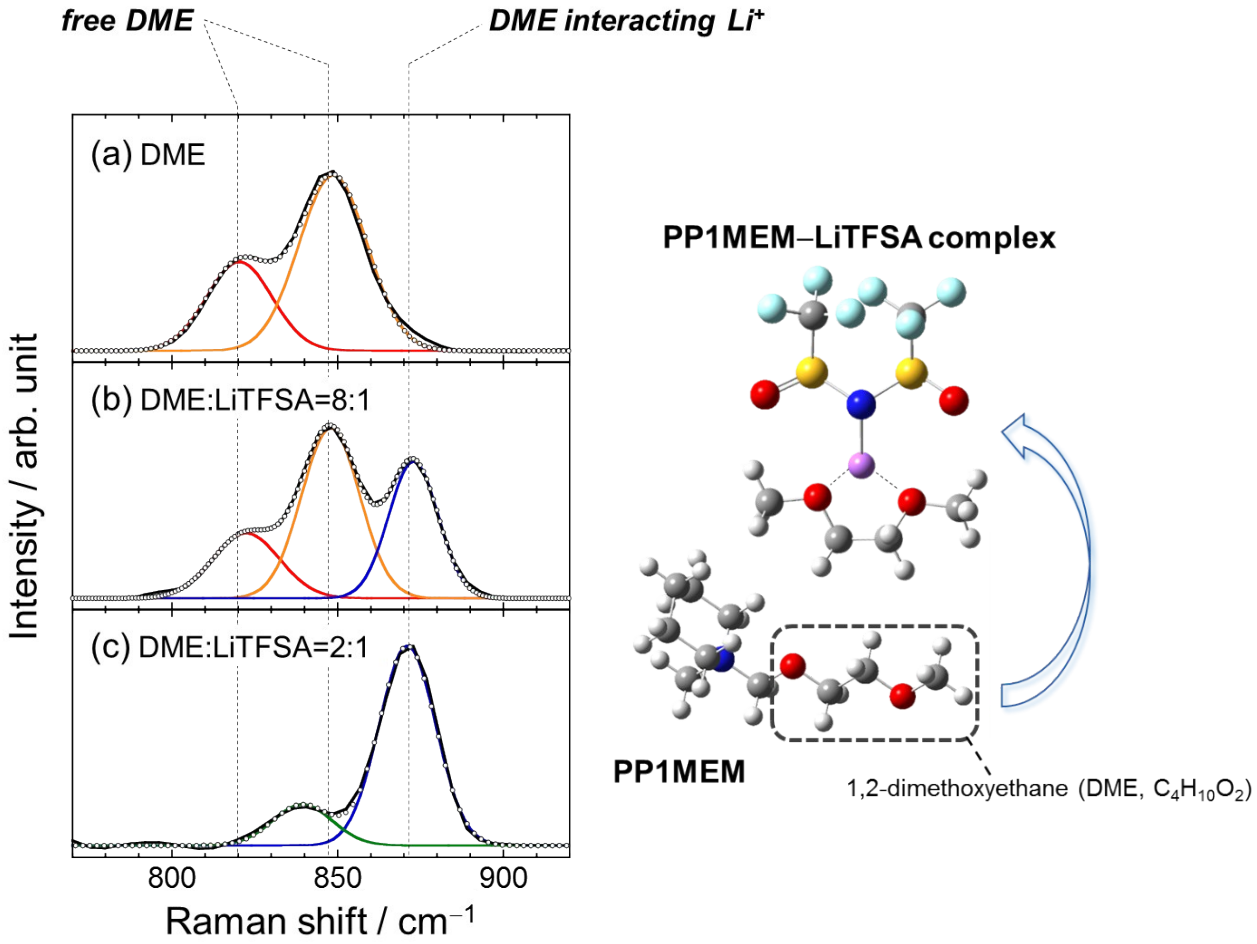

Figure S5. Raman spectra of (a) pure DME solvent and DME–LiTFSA solutions. The molar ratios of DME to LiTFSA are (b) 8:1 and (c) 2:1, respectively. Schematic illustration of proposed structure of PP1MEM–LiTFSA complex based on the results of the Raman measurements was shown.

Raman spectra of $(LiTFSA)_x(Ionic\ liquid)_{1-x}$ solutions (x = 0, 0.1, 0.2)

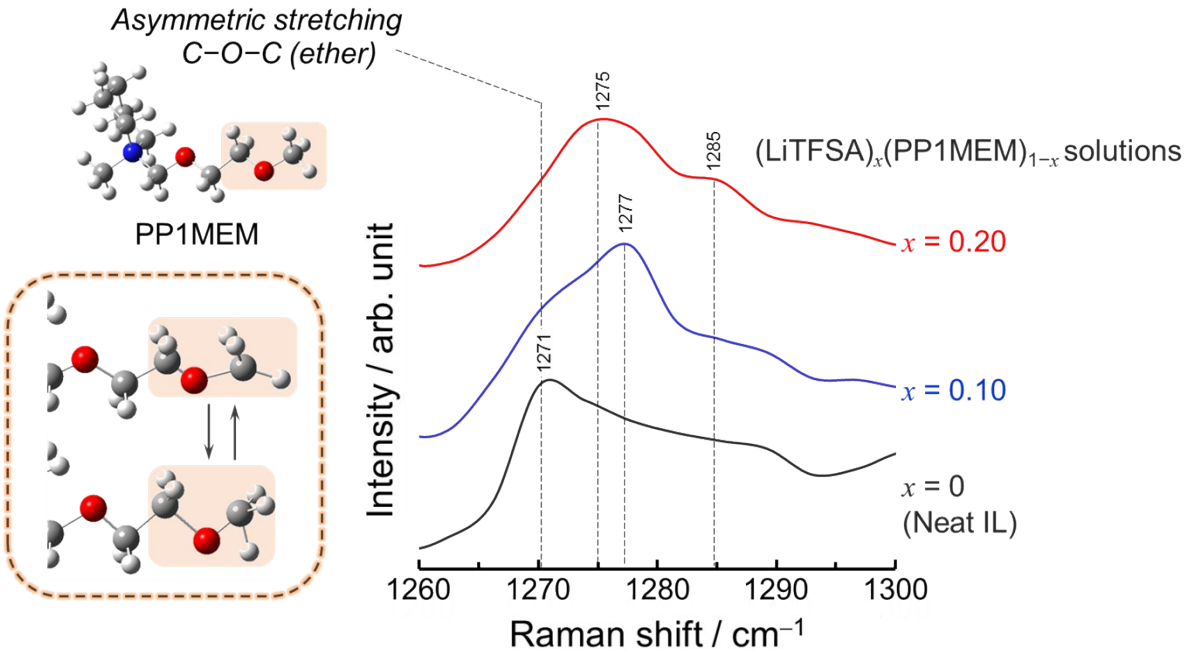

Figure S6. Raman spectra of $(LiTFSA)_x(PP1MEM\text{-}TFSA)_{1-x}$ (x = 0, 0.10 and 0.20) in the frequency range of 1260 to 1300 cm^{-1} (finger region). The electrolyte solutions were put into a quartz cell, and tightly sealed in it within an argon atmosphere to avoid an effect of water in air.

We searched a signature of interaction between Li ion and ether moiety of PP1MEM from Raman spectra of the $(LiTFSA)_x(PP1MEM\text{-}TFSA)_{1-x}$ solutions (x = 0, 0.10 and 0.20). Figure S6 displays the Raman spectra in the range of 1260 to 1300 cm^{-1} (fingerprint region). Neat PP1MEM-TFSA showed the asymmetric stretching ν(C−O−C) vibration coupled with C−H vibration at 1271 cm^{-1}. When LiTFSA was added to the pure ionic liquid with a molar fraction of 0.10, the band intensity was relatively reduced, and the additional band was appeared in a high wavenumber side of 1277 cm^{-1}. A band associated with molecular solvents typically shifts to high wavenumber side upon binding of the solvent molecules to metal ions. It is inferred that the ether side chain of PP1MEM cation became rigid

by the interaction of the ether moiety with Li ion (coordination of Li ion into the ether moiety). This is probably the reason for the reduced band intensity (1271 cm^{-1}) and the appearance of the new band (1277 cm^{-1}). At a further addition of LiTFSA (x = 0.25), however, a band located at 1275 cm^{-1} also observed. It is expected that the configuration of PP1MEM cation surrounded by TFSA anions is very complicated, so that what the band means is still unclear. As one hypothesis, we guess that the band indicates the stabilization of PP1MEM-LiTFSA at a certain molar fraction. In a future study, we will investigate what the bands show by computational chemistry support.

Solvation number of PC solvent per Li-ion in LiTFSA–PC solutions

Raman spectra of pure PC solvent and LiTFSA–PC solutions with various concentration from 0.5 to 2.0 mol dm^{-3} (M) are displayed below. The bands at 710 cm^{-1} and 739 cm^{-1} is assigned to the symmetric deformation mode of "*free*" PC molecules and CF_3 bending vibration δ_s (CF_3) coupled with the S−N stretching vibration ν_s (S−N−S) of TFSA anions, respectively. By dissolution of LiTFSA-salt in PC solvent, the new band appears at 721 cm^{-1}, which is attributed to the PC solvating Li ion. The average solvation numbers of PC solvents (N_{PC}) per Li ion can be determined by the following equations[1,2]:

$$\frac{C_{free}}{C_{solv}} = \frac{I_{free}}{I_{solv}} \cdot \frac{\Gamma^*_{solv}}{\Gamma^*_{free}} \qquad (1)$$

$$I_{solv} = -\frac{\Gamma^*_{solv}}{\Gamma^*_{free}} I_{free} + C_{PC,tot}\Gamma^*_{solv} \qquad (2)$$

$$N_{PC} = \frac{C_{solv}}{C_{Li,tot}} = \frac{C_{PC,tot}}{C_{Li,tot}(1 + C_{free}/C_{solv})} \qquad (3)$$

where Γ^*_{free}* and Γ^*_{solv} denote Raman intensities per unit concentration of the free PC and the PC solvating Li ion, respectively. (Total concentration of PC; $C_{PC,tot} = C_{free} + C_{solv}$)

Reference

(1) M. Morita, Y. Asai, N. Yoshimoto, and M. Ishikawa, *J. Chem. Soc., Faraday Trans*., 1998, **94**, 3451−3456.

(2) Y. Yamada, Y. Koyama, T. Abe, and Z. Ogumi, *J. Phys. Chem. C*, 2009, **113**, 8948–8953.

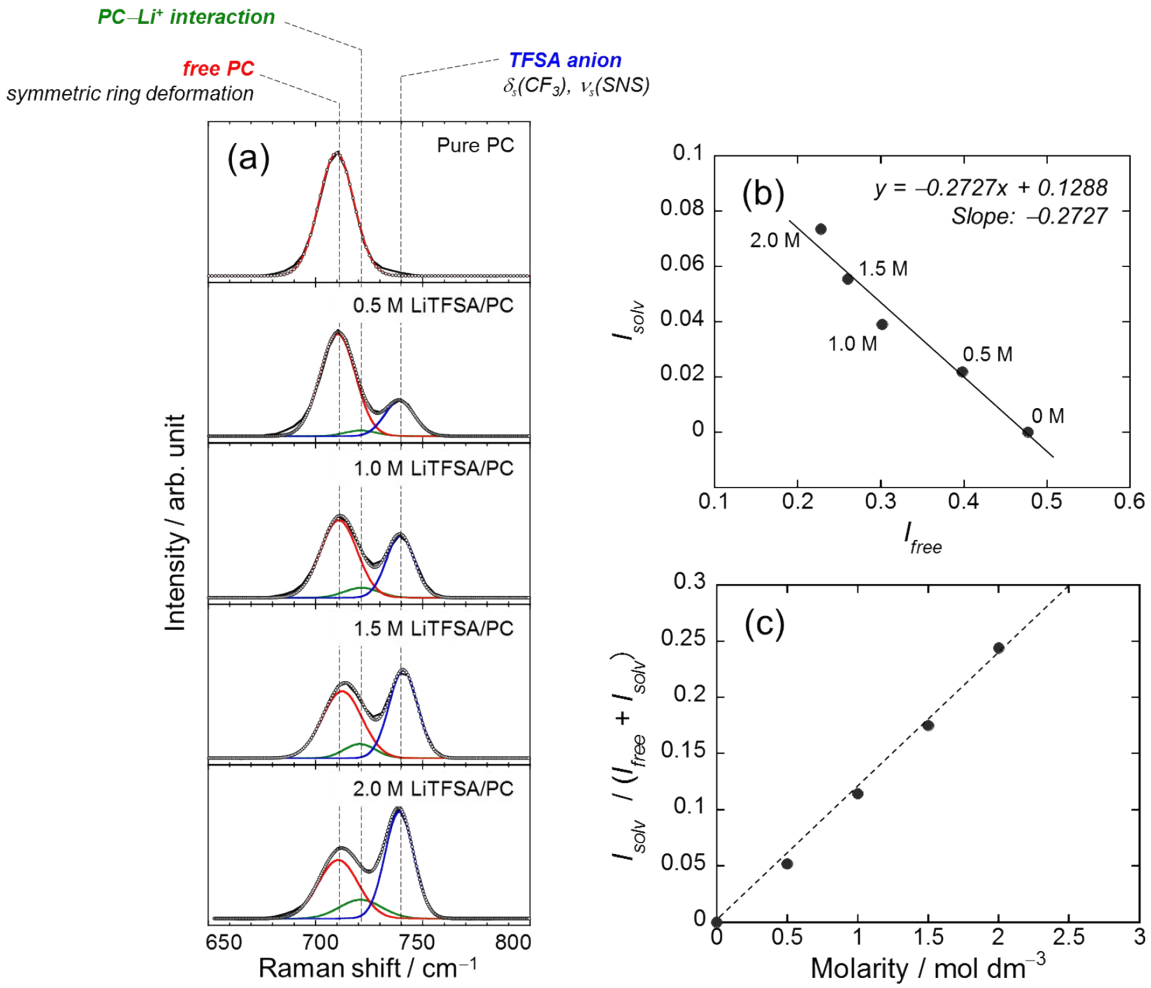

Figure S7. (a) Raman spectra of pure propylene carbonate (PC) solvent and electrolytes consisted of LiTFSA and PC with various concentration (0.5, 1.0, 1.5, 2.0 M). (b) Relation between the intensities of free PC (I_{free}) and PC solvating Li^+ (I_{solv}) in the 0.5−2.0 M LiTFSA/PC electrolytes. (c) Plot of I_{solv} / (I_{solv}+ I_{free}) versus molarity of LiTFSA.